PHOTODISINTEGRATION OF HELIUM, I.

A. N. GORBUNOV and V. M. SPIRIDONOV

P. N. Lebedev Physics Institute, Academy of Sciences, U.S.S.R.

Submitted to JETP editor February 11, 1957

J. Exptl. Theoret. Phys. (U.S.S.R.) 33, 21-32 (July, 1957)

The photodisintegration of helium was studied with a cloud chamber located in a magnetic field and synchronized with a 170 Mev bremsstrahlung beam. The yields of the different photonuclear reactions on helium were determined. The energy dependence of the cross section and the angular distributions of the protons and the tritons were measured for the reaction $He^4(\gamma, p)H^3$. The results are compared with data obtained in other investigations and with theoretical predictions.

1. INTRODUCTION

THE investigations of high energy photoprotons and photoneutrons emitted from different nuclei[1-7] have demonstrated many characteristics of these processes (asymmetry of angular distributions, forward shift of the maximum in the angular distribution with increasing photon energy, large size of the isotropic component, the presence of distinct peaks in the energy spectrum of the photoprotons, etc.). Many different models of photon-nucleon interaction have been proposed to explain the different phenomena. In particular, for photon energies > 100 Mev the experiments are satisfactorily described by the pseudo-deuteron model.[8,9] At lower energies the angular distributions of protons according to Yoshida[10] are better in agreement with absorption in α-subunits of nuclei.

The α-particle model of nuclear γ-absorption has earlier also been suggested by Levinger and Bethe[11] to explain the characteristics of the giant resonance of the photonuclear reactions. In order to develop this model further it is useful to study the photodisintegration of free α-particles.

The photodisintegration of helium is of interest also from other considerations. Contrary to the case of more complicated nuclei, it is possible in the case of helium to analyze fully the angular distributions and consequently to draw conclusions on the character of the photon absorption. This is due to the fact that the final state in the (γ, p) and (γ, n) processes (the fundamental photonuclear reactions in He) is a two-body system [$p + H^3$ in the (γ, p) process and $n + He^3$ in the (γ, n) process], and both H^3 and He^3 do not have excited states.

Furthermore, by studying the energy dependence of the (γ, p) and (γ, n) reactions (which is also considerably simplified by the above mentioned circumstances) one can obtain the energy dependence of the photon absorption cross section. This allows one then to determine the integrated cross section as well as the mean and the harmonic mean energy of photon absorption. Comparing these with the theoretical expressions derived in several papers by use of the sum rule [11-13] one can estimate the contribution of exchange forces to the integrated absorption cross section. By comparing the experimental curves of the cross sections of the (γ, p) and (γ, n) reactions with theoretical predictions found for example in Ref. 14 one can obtain information on the wave functions of the α-particle, H^3, and He^3.

Finally, $He^4(\gamma, p)H^3$ and $He^4(\gamma, n)He^3$ are mirror reactions in iso-space. Therefore a comparison of these reactions will allow one to draw conclusions on the interaction operator between the electromagnetic field and the nucleus.

Up to now only very few experiments on the disintegration of helium have been performed despite the considerable importance of this reaction. Fuller[15] investigated the (γ, p) reaction by observing proton tracks in nuclear emulsions. In his experiment the plates were placed inside a target chamber containing helium gass which was irradiated with x-rays of 40 Mev maximum energy. With the same method De Saussure and Osborne[16] sutided the (γ, n) reaction observing the He^3 recoils; their maximum photon energy was 150 Mev. Gaerttner and Yeater[17] studied the photodisintegration of helium with a cloud chamber (without a magnetic field) with a bremsstrahlung spectrum of $E_{\gamma\ max} = 100$ Mev. At an energy of

300 Mev, Benedict and Woodward[18] studied high energy photoprotons with scintillation counters while Kikuchi[19] used nuclear emulsions under similar conditions. Goldwasser and Nicolai[20] published a short communication on an experiment of the photodisintegration of helium above the meson threshold.

The above experiments were performed at different energies and in different experimental arrangements, and usually in a way which allowed only one of the reactions occurring in the photodisintegration of helium to be observed. Their results on the angular distributions and energy dependence of the (γ, p) and (γ, n) reactions cannot therefore be reliably compared. Furthermore, they do not give information on the other possible reactions. We therefore undertook the investigation of the photodisintegration of helium with a cloud chamber in a magnetic field. The x-ray spectrum had a maximum energy of 170 Mev. We chose a cloud chamber since this was the only method available allowing simultaneous observation of all the reactions occurring in the photodisintegration of helium. In the present paper we shall give the results of the (γ, p) reaction and some results concerning the other reactions. Detailed results on the reactions $He^4(\gamma, pn)H^2$ and $He^4(\gamma, n)He^3$ will be presented later.

2. EXPERIMENTAL ARRANGEMENT

The special considerations connected with the use of a cloud chamber in an x-ray beam from a synchrotron and the apparatus connected with such a work were discussed earlier.[21,22] We shall therefore limit ourselves to a short description of the experimental arrangement (see Fig. 1).

The collimated bremsstrahlung beam of the synchrotron of the Physics Institute of the Academy of Sciences was first cleaned from electron contamination with a sweeping magnet. It entered the sensitive region of the cloud chamber through a thin window made of cellulose triacetate. The cloud chamber had a diameter of 30 cm and a depth of 8 cm. In order to decrease the electron background the beam travelled between the sweeping magnet and the cloud chamber through an evacuated pipe. The expansion of the cloud chamber was synchronized with the yield pulse of the synchrotron in an appropriate way. Pictures were taken at 55 sec intervals. The applied magnetic field had a strength of 5500 gauss. The inhomogeneity of the field did not exceed 2% over the sensitive region of the cloud chamber.

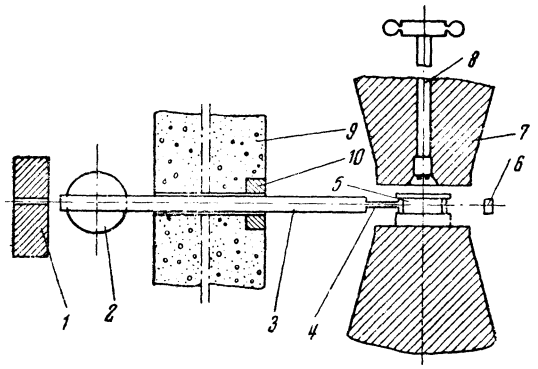

FIG. 1. Diagram of the experimental setup. 1 — lead collimator, 2 — sweeping magnet, 3 — evacuated tube, 4 — beam entrance arrangement into the cloud chamber, 5 — cloud chamber, 6 — pulsed ionization chamber, 7 — magnet, 8 — stereoscopic camera, 9 — concrete wall, 10 — lead absorber.

To monitor the yield of only those x-ray bursts which resulted in a picture, the ionization chamber placed in the x-ray beam was pulsed at the appropriate burst. The chamber was calibrated in terms of intensity in an absolute way utilizing the β^+ activity induced in a carbon sample by the reaction $C^{12}(\gamma, n)C^{11}$; the absolute value of this cross section was taken from Ref. 23. The procedure of calibration of an ionization chamber has been described in Ref. 22. The calibration of our chamber was performed twice during the experiments and the results of the calibration agreed within the experimental accuracy of 2%.

3. ANALYSIS OF THE PICTURES

The obtained cloud chamber pictures where treated in the following sequence: (a) the pictures were scanned; (b) all nuclear reactions due to γ-quanta were identified; (c) the events to be analyzed were selected and the lengths of the projection of the tracks, the radius of curvature, and the angle of emission with respect to the direction of the x-ray beam were determined. All films were scanned twice. Ordinary stereoscopes were used for this purpose. Furthermore, all unclear or spoiled events were scrutinized on a 30× microscope (type UIM-21). This scanning procedure practically eliminated the possibility that any reaction has been overlooked.

One can classify all near reactions observed in a gas cloud chamber according to the number of emit-

ted visible tracks, i. e., according to the number of charged particles in the final state. Since the maximum energy of the x-rays used in this experiment (170 Mev) was insufficient to create a charged meson in addition to disintegrating helium, all reactions with three or more tracks had to be due to the oxygen and carbon impurities.

The following reactions lead to two charged particles:

$$He^4 + \gamma \to p + H^3, \quad (1)$$

$$He^4 + \gamma \to d + d, \quad (2)$$

$$He^4 + \gamma \to p + n + d, \quad (3)$$

$$He^4 + \gamma \to p + p + n + n, \quad (4)$$

$$I + \gamma \to p + \text{recoil nucleus} \quad (5)$$

$$I + \gamma \to p + n + \text{recoil nucleus} \quad (6)$$

Here I stands for an impurity nucleus present in the chamber other than helium (C or O).

In the reactions (1), (2) and (5) the final state is a two body state. Therefore the particles in the center of mass system go in opposite directions, and the tracks are complanar with the incoming photons. In the laboratory system the angle between the tracks is not smaller than 160°. With these characteristics one can distinguish between the reactions (1), (2), (5) on the one hand and (3), (4), (6) on the other. The (γ, p) (see Fig. 2) and the (γ, 2d) reactions give tracks with different relative ionization density. In reaction (1) the ionization due to the H^3 is considerably greater than that due to the proton (5 — 9 times depending on the angle of emission), while the ionization density of both tracks is roughly the same for reaction (2). The reactions of the I(γ, p) type are distinguished by the very great difference between the ionization density of the two tracks (see Figs. 2 and 3); the track of the recoil nucleus always ends inside the chamber. This way it is possible uniquely to distinguish between (γ, p) reactions in helium and in the impurity nuclei. In the reactions (3), (4) and (6) (see Fig. 3) the outgoing particles may leave with arbitrary angles with respect to each other and the direction of the incoming x-rays. The reaction I(γ, np) can be distinguished from the reaction $He^4(\gamma, pn)H^2$ in the same way as I(γ, p) from $He^4(\gamma, p)H^3$.

One charged particle is emitted in the following reaction:

$$He^4 + \gamma \to n + He^3, \quad (7)$$

$$I + \gamma \to n + \text{recoil nucleus} \quad (8)$$

Furthermore, the elastic production of π^0-mesons, $He^4(\gamma, \pi^0)He^4$, is energetically possible. However, one can neglect contributions from this reaction, in accordance with the estimated small probability of this event.

The yields from the reaction I(γ, p), I(γ, pn) and I(γ, n) were determined under similar operating conditions with a filling of the cloud chamber with hydrogen instead of helium. The following ratio for the yields was obtained: $I(\gamma, n)/[I(\gamma, p) + I(\gamma, pn)] = 0.57$. When the chamber is filled with helium one can obtain from the number of the observed reactions I(γ, p) and I(γ, pn) the number of the reactions I(γ, n). Subtracting this number from the total number of observed reactions with one charged particle one obtains the number of (γ, n) reactions in helium.

To obtain the angular distributions and the energy dependences one has to know the momenta of the particles and the angles of emission with respect to the direction of the incoming γ-quantum. For the determination of these quantities tracks were used whose projection on the bottom of the cloud chamber had a length ≥ 53 mm. It was not possible to measure with sufficient accuracy the radius of curvature for shorter tracks. When restricting oneself to still longer tracks some accuracy is gained, on the one hand, in the determination of the curvature, but on the other hand the statistical accuracy is then reduced and a low γ-ray energy region in the yield curves is cut off.

The projections of the angles between the tracks and the incoming γ-rays were determined with a microscope of the UIM-21 type. The error in this determination was less than 0.5°. The actual angles were obtained from the projected angles by the relation

$$\theta = \arccos\{\cos\alpha / \sqrt{1 + (h/l)^2}\},$$

where θ is the angle of emission of the particle, α its projection on the plane of the camera, 2h the height of the illuminated region, and ℓ the length of the projection of the track. Under the conditions of the present experiment the difference between θ and α is significant only for small angles with the beam direction and for small ℓ.

The radii of curvature were determined by comparing the tracks with standard circles. This method is very fast and sufficiently accurate up to radii of curvature of 200 — 300 cm. The radii of curvature were independently determined twice. The average deviations of the measurements were 3 — 5%. In the final results a correction was added to take into account the momentum parallel to the magnetic field.

Since in the reaction $He^4(\gamma, p)H^3$ the final state has only two particles it is possible to determine the energy of the γ-quantum from the emission angle and momentum for only one of the outgoing particles. By measuring both tracks one can therefore check the correctness of the measurement. The calculations were performed by means of nomograms, one for protons and one for tritons. For known momentum and emission angle in the laboratory system they gave the energy of the photon and the angle of emission in the center-of-mass system. The construction of such nomograms is straightforward. For a given photon energy E_γ one finds the momentum of the particle due to the c.m.s. momentum p_0, and the momentum p_c in the c.m.s. Then the momentum in the laboratory system is $p_{lab} = p_0 + p_c$. p_c depends only on E_γ and not on the kind of particle, while p_0 depends both on E_γ and on the mass of the particle. Such nomograms are shown in Fig. 4. Each half circle corresponds to a given photon energy, and the radial curves correspond to given angles in the c.m.s.

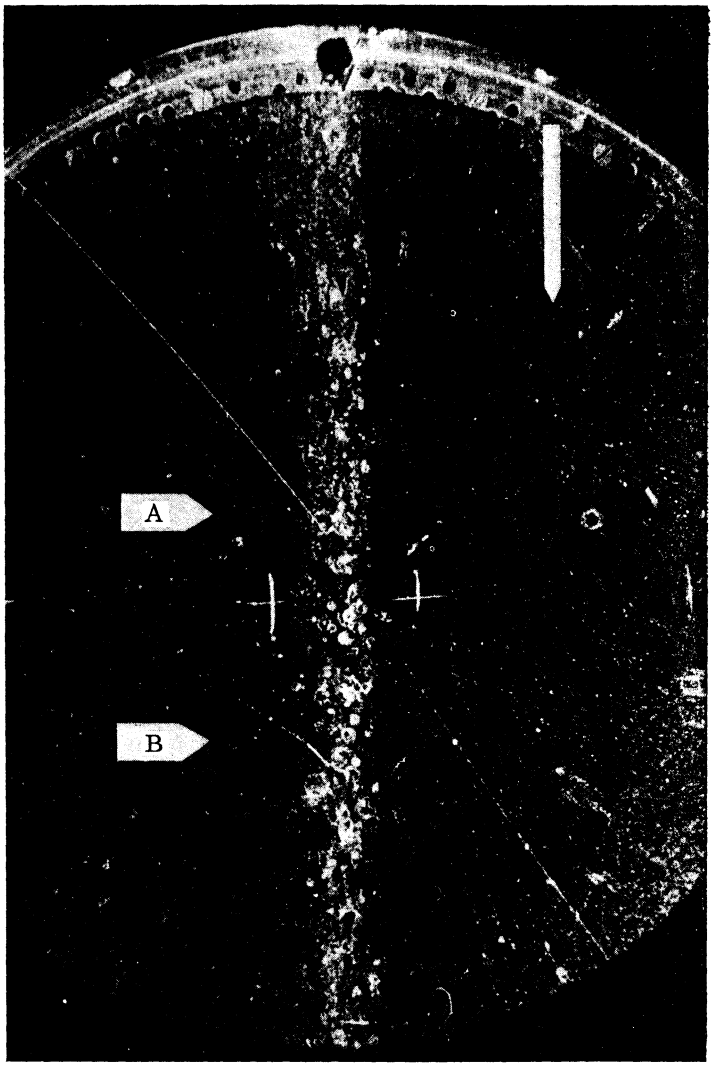

FIG. 2. A — reaction $He^4(\gamma, p)H^3$. The proton travels forward, the triton backward (the direction of the incoming photon beam is indicated by the arrow). B — (γ, p) reaction with impurity nucleus; the heavy short track belongs to the recoil nucleus.

The above method was used to measure 742 proton tracks and 709 triton tracks. All these data were entered on nomograms, protons and tritons separately, to obtain the angular and energy distributions in the c.m.s. The number of points falling into each interval are given in Fig. 4. Since only tracks with length ≥ 5.3 cm were measured there are no points in the nomograms for $E_\gamma < 21$ Mev for protons and $E_\gamma < 30$ Mev for tritons. The nomogram is drawn only for $E_\gamma \leq 70$ Mev.

Owing to the limited height of the illuminated region, only a certain fraction of the particles emitted at an angle θ with respect to the direction of the γ-quantum beam have been measured. This fraction depends on θ. To obtain the actual number of particles emitted at an angle θ from the number of tracks having projections ≥ 5.3 cm it is therefore necessary to apply the correction factor

$$k(\theta) = \frac{\pi}{2 \arcsin(\sin\theta_0/\sin\theta)},$$

where $\tan\theta_0 = (h/5.3)$ and 2h is the height of the illuminated region. The coefficients $k(\theta)$ vary almost linearly with θ in different θ intervals even for large changes in h. Therefore a change of the illuminated region will have a very small influence on the angular distributions and an even smaller influence on the energy distributions. To obtain the angular distributions the measured quantities have to be related to

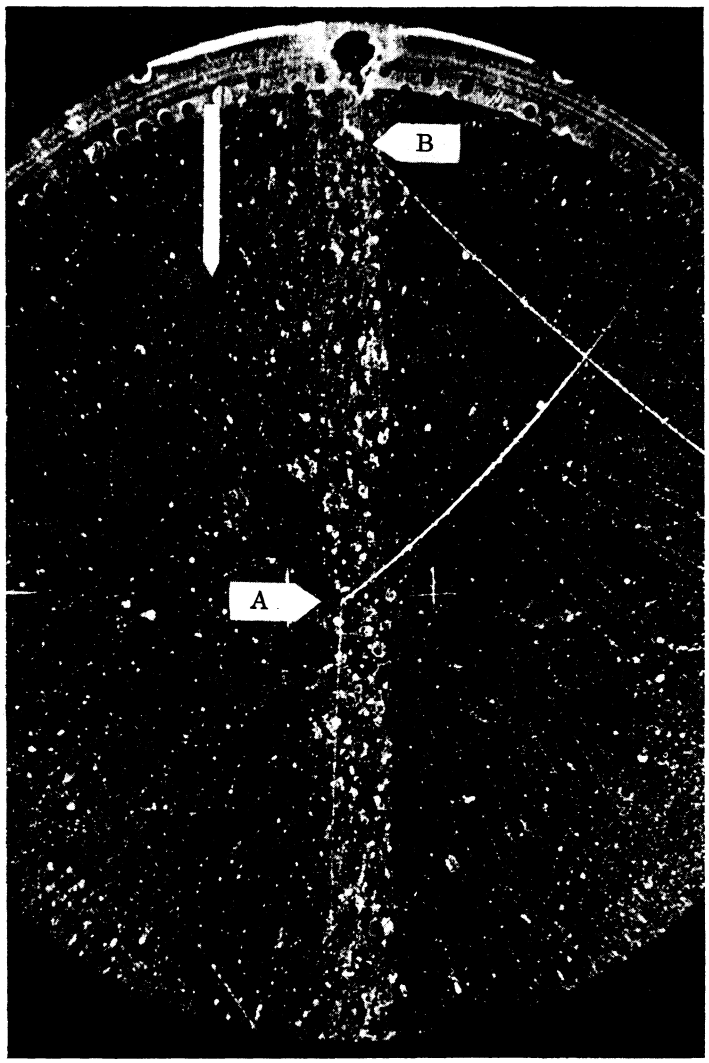

FIG. 3. A— reaction $He^4(\gamma, pn)H^2$. The proton travels forward, the deuteron backward (the direction of the incoming photon beam is indicated by the arrow). B — (γ, p) reaction with impurity nucleus; the heavy short track belongs to the recoil nucleus.

unit solid angle. The experimental numbers therefore were multiplied by $\kappa(\theta) = k(\theta)/\Omega(\theta)$.

To check the correctness of the assumed depth of the illuminated region and consequently the correctness of $k(\theta)$ and $\kappa(\theta)$ the total number of observed (γ, p) events was compared with the total number of protons, determined from the nomogram and corrected with $k(\theta)$. Further, in this comparison it had to be taken into account that the events due to photons of energy between the reaction threshold (19.8 Mev) and 21 Mev were not included in the nomogram.

4. RESULTS OF THE MEASUREMENTS

The total numbers of photonuclear reactions on helium are given in Table I. They were obtained from 9000 cloud chamber pictures.

The analyzed events due to (γ, p) reactions and falling within the indicated ranges of photon energy and center-of-mass emission angles are shown in the nomogram, Fig. 4. Only tracks whose projection of the track lengths was ≥ 5.3 cm were utilized. This was done both for protons and for tritons. These numbers together with the known number of helium nuclei per unit volume in the cloud chamber and the known integrated photon flux through the chamber, along with the correction factors $k(\theta)$ and $\kappa(\theta)$ respectively, yield the energy dependence of the (γ, p) cross section (Fig. 5) and the angular distributions for photon energies 21 — 30 Mev and 30 — 170 Mev (Fig. 6). These two energy ranges for the angular distribution were chosen using the ratios $N_p(0 - 90°)/N_p(90 - 180°)$, given in Table II. Here $N_p(0 - 90°)$ and $N_p(90 - 180°)$ are the number of protons emitted in the c.m.s. in the forward and the backward hemispheres respectively.

TABLE I

Reaction	Number of observed curves	Yield relative to the (γ, p) reaction
$He^4(\gamma p)\,H^3$	2835	1
$He^4(\gamma n)\,He^3$	2685	0.95 ± 0.04
$He^4(\gamma pn)\,d$ + $+He^4(\gamma 2p2n)$	547	0.19 ± 0.01
$He^4(\gamma 2d)$	$\leqslant 59$	$\leqslant 0.02$

As can be seen from Table II, a sharp change occurs in the angular distributions of the protons at a photon energy 30 — 35 Mev. The angular distributions obtained independently from proton and from triton tracks are plotted separately. They agree within the statistical accuracy. This indicates the correctness of the measurements.

5. ERRORS OF MEASUREMENT

(a) The error in the true spatial angle is due to the inaccuracy with which the correction for the dip angle has been performed, and due to the neglect of the fact that the photographic picture is the result of a conical projection and not a parallel projection. One can show that the rms errors introduced this way

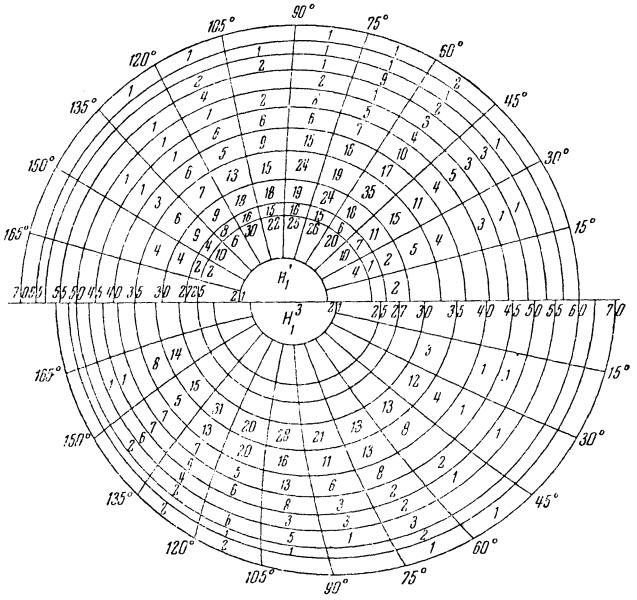

FIG. 4. Nomogram for the determination of the energy and angular dependence of the $He^4(\gamma, p)H^3$ cross section: from proton tracks (upper half) and from H^3 tracks (lower half).

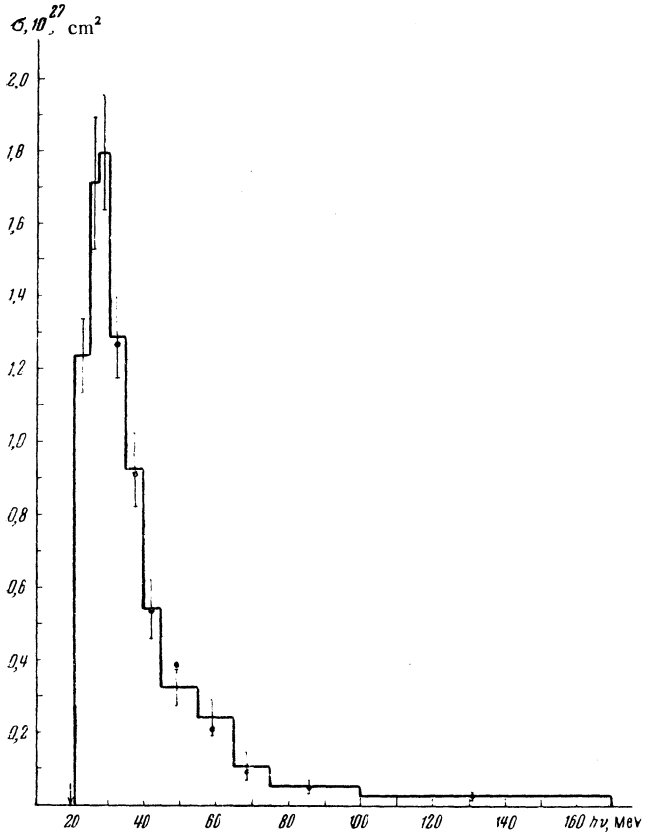

FIG. 5. Energy dependence of the cross section for the reaction $He^4(\gamma, p)H^3$ as determined from proton tracks. Only the statistical uncertainties are indicated. The threshold (19.8 Mev) is indicated by the arrow. The cross sections obtained from triton tracks are indicated by the full circles.

do not exceed ±3.5° for each track. Since this error is statistical in character it practically does not show up in the numbers of tracks falling into a particular angular interval (each interval was chosen to be 15°).

(b) The error in the determination of the energy of the photon responsible for a (γ, p) reaction is compounded of the following parts: errors in the determination of the magnetic field strength, errors due to the nonuniformity of the magnetic field and due to the fluctuations in the magnetizing current, and, finally, errors in the curvatures of the emerging particles and in the angles with respect to the beam and to a plane perpendicular to the magnetic field. The magnetic field was measured with a fluxmeter which was calibrated at two field values in a standard field determined by nuclear magnetic resonance. The total error in the field measurements was ± 0.5%.

The rms error associated with the measurement of curvatures and angles was determined by obtaining the energy of the photon from the two emitted tracks separately. The magnitude of these errors changes between 2.5 and 4% depending on the energy of the photon (this error obviously includes the influence of the inhomogeneity of the magnetic field).

(c) The error in the absolute value for the intensity of the radiation is compounded of the following parts: (1) errors in the calibration of the ionization chamber in terms of the activity of the carbon sample and errors due to apparative instabilities; (2) errors in the determination of the absolute activity of the carbon sample, and (3) errors in the quantity $\int \sigma_{\gamma n}(W)\,\eta(W)\,dW$ where $\eta(W)$ is the bremsstrahlung spectrum. Error (1) was determined by performing the

TABLE II

Ratio $N_p(0-90°)/N_p(90-180°)$ for protons

Photon energy Mev	From proton tracks	From triton tracks
21—25	1.10	—
25—27	0.93	—
27—30	1.21	—
30—35	1.96	2.04
35—40	2.34	1.89
40—170	2.48	2.70
Below 30	1.09±0.13	—
Above 30	2.23±0.26	2.23±0.30

calibration twice. It was found to be ± 2.0%. Error (2) does not exceed 5% according to Ref. 24. Our measurement of the yields of the (γ, n) and (γ, p) reactions in C and O which entered the working mixture of our cloud chamber confirmed in a qualitative manner the absolute activity determination of the carbon sample. According to Ref. 23 error (3) has a magnitude ± 2%. The total rms error in the determination of the absolute intensity of the radiation is 6%.

6. DISCUSSION OF THE RESULTS

Yields of Photonuclear Reactions in Helium

The yields of the different possible photonuclear reactions in helium relative to the (γ, p) reaction are given in Table I. It can be seen that within experimental accuracy the yields for the (γ, p) and (γ, n) reactions are the same while the yield for the (γ, 2d) reaction does not exceed 2% of the yield of the (γ, p) reaction. These results are as expected since both (γ, n) and (γ, p) reactions are allowed in a dipole transition and have practically equal cross sections (neglecting the slight difference in the thresholds and in the Coulomb barrier). On the other hand, a dipole transition is forbidded for the (γ, 2d) reaction because of isotopic spin selection rules.

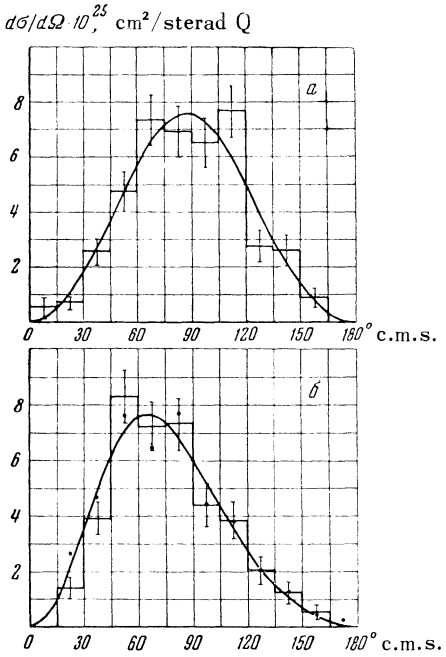

FIG. 6. Angular distributions of the protons from the reaction $He^4(\gamma, p)H^3$ in the c.m.s. (a) proton energy 21 — 30 Mev; (b) 30 — 170 Mev. In (b) the full circles indicate the proton angular distribution inferred from the measurements on triton tracks. The full curves represent Eq. (9).

The experiments in Refs. 17, 20 were also performed with cloud chambers. They yielded for the (γ, n)/(γ, p) yield ratio the values 1.3 and 1.8 respectively. (In Ref. 17 this ratio is based on 59 single tracks which were assumed to belong to the (γ, n) reaction, and on 45 tracks from the (γ, p) reaction; in Ref. 20 the number of events was not given.) This large (γ, n)/(γ, p) ratio, besides being based on a small statistical sample, could possibly be connected with operation of the cloud chamber at lower sensitivity in order to decrease the electron background. As a result of this there may have been lost some proton tracks from the (γ, p) reaction which then would be counted as a (γ, n) reaction.

The yield of the (γ, pnd) reaction comprises about 9% of the reaction leading to two particles in the final state, for photon energies 20 to 170 Mev. From the preliminary results of this experiment it seems that this reaction has the character of the pseudo-deuteron effect.

Energy Dependence of the (γ, p) Cross Section

As can be seen from Fig. 7, the cross section for the (γ, p) reaction in helium has a resonance-like shape with a maximum cross section ~ 1.8×10^{-27} cm² at a photon energy 27 — 28 Mev. The halfwidth is around 15 Mev. For a photon energy $E_\gamma \geq 35$ Mev the energy dependence of the cross section is well represented by a function of the form $E_\gamma/(E_\gamma - \epsilon)^{2.5}$. On Fig. 7 there are also shown the cross sections for the (γ, p) reaction obtained by Fuller[15] with a photon spectrum of maximum energy of 40 Mev. In this experiment there had to be made large corrections due to the fact that triton and He^3 tracks could sometimes not be distinguished from proton tracks. The results for photon energies between threshold and 26 Mev therefore are not too reliable. Fuller's cross section shows a maximum at the energy 26 Mev and has there a magnitude in agreement with the present experiment. However, his halfwidth is ~ 10 Mev, i. e., somewhat smaller than our halfwidth.

In Fig. 7 there further are given points obtained from the cross section of the inverse reaction $H^3(p, \gamma)He^4$ from Ref. 25. This experiment covers proton energies up to 6.5 Mev. These points are in good agreement with the present experiment. The dashed curve of Fig. 7 is a theoretical curve for the absorption cross section for dipole radiation given by Gunn and Irving.[14] In this paper the nuclei He^4 and H^3 were described by exponential wave functions with the parameters $1/\mu_\alpha = 1.7 \times 10^{-13}$ cm and $1/\mu_T = 2.5 \times 10^{-13}$ cm. They were determined to give the correct binding energy for He^4 and the correct Cou-

lomb energy for He^3. The motion of the proton and triton in the final state were described by plane waves. In this calculation noncentral forces were not taken into account.

One sees from Fig. 7 that the experimental cross sections decrease with increasing energy much faster than the theoretical cross section of Gunn and Irving.

The integrated cross sections for the reaction $He^4(\gamma, p)H^3$ obtained from our curve are given in Table III together with those found by the other workers. One sees from this Table that the energy interval 40 — 170 Mev (i.e., the region far removed from the resonance) contributes a considerable fraction (~ 34%) to the integrated cross section.

Taking into account that the yield and also the position of the maximum for the reaction $He^4(\gamma, n)He^3$ are approximately the same as in the (γ, p) reaction one can expect* that the integrated cross section for the (γ, n) reaction will be close to that of the (γ, p) reaction. For the integrated cross section of the reaction $He^4(\gamma, pn)H^2$ we have obtained the value 10.0 ± 1.4 Mev.mb. With these data one can make a preliminary discussion of the integrated photon absorption cross section of the helium nucleus.

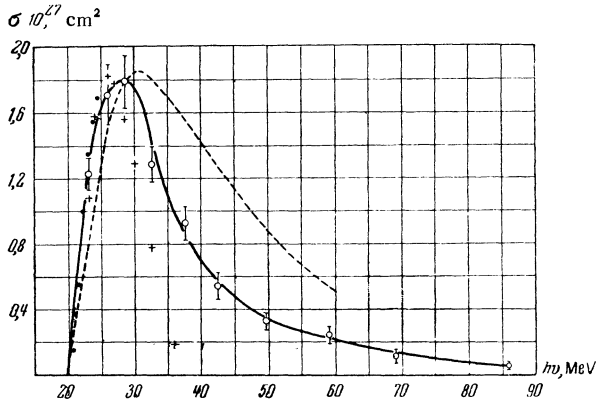

FIG. 7. Comparison of the cross section of the reaction $He^4(\gamma, p)H^3$ with the data of other investigations. Open circles and solid curve drawn through these — results of the present work; crosses — Fuller's[15] points; full circles — inferred from the inverse reaction $H^3(p, \gamma)He^4$ as per Perry and Bame;[25] dotted curve — theoretical curve for the cross section calculated by Gunn and Irving[14] employing an exponential wave function for He^4 and H^3 with $1/\mu_\alpha = 1.7 \times 10^{-13}$ cm and $1/\mu_T = 2.5 \times 10^{-13}$ cm.

$$\sigma_{int} = \int_0^{170} \sigma(W)\, dW = 2\sigma_{int}(\gamma p) + \sigma_{int}(\gamma pnd) + \\ + \sigma_{int}(\gamma\, 2p\, 2n) + \sigma_{int}(\gamma 2d) = 88 \pm 7 \text{ Mev.mb}$$

This value can be compared with the sum rule calculation of Levinger and Bethe[11] of the integrated electric dipole absorption cross section which included the effects of exchange forces:

$$\int \sigma(W)\, dW = 0.015 \cdot A\,(1 + 0.8x) \text{ Mev.bn}$$

where x is the fractional strength of the exchange forces. This expression yields for helium with x = 0.5 the value $\int \sigma(W)\, dW$ = 84 Mev.mb which agrees well with the experimental value 88 ± 7 Mev.mb.

In a similar way one can evaluate a different moment of the photodisintegration cross section of helium

$$\sigma_b = \int \frac{\sigma(W)}{W}\, dW,$$

For this quantity we obtain from our experiment the value $\sigma_b = 2.40 \pm 0.15$ mb. This quantity is connected with the rms radius of the nucleus. It was shown in Ref. 26 that for electric dipole transitions holds

$$\int \frac{\sigma_{E_1}(W)}{W}\, dW = \frac{4\pi^2}{3}\left(\frac{e^2}{\hbar c}\right)\frac{NZ}{A-1}\,(1 - \Lambda)\int \rho(r)\, r^2 d\tau,$$

where r is the distance from the center of mass of the nucleus, and $\rho(r)$ is the charge density of the nucleus normalized to $\int \rho(r)\, d\tau = 1$. The value of Λ takes the inequality of the nucleons into account. This inequality can be due only to the Coulomb energy or the Pauli principle. In He^4 the Coulomb forces are small and there are no restrictions from the Pauli principle. Therefore for He^4 we have $\Lambda = 0$. If $\rho(r)$ is constant we have

$$\int \rho(r)\, r^2 d\tau = \frac{3}{5} R^2,$$

where $R = r_0 A^{1/3}$. This yields for helium

*Our results on the (γ, n) reaction are being at present analyzed. The results will be reported at a later date.

$$\int \frac{\sigma_{E_1}(W)}{W} dW = \frac{4\pi^2}{5}\left(\frac{e^2}{\hbar c}\right) \cdot \frac{4}{3} R^2.$$

With the experimentally obtained value $\sigma_b = 2.4 \pm 0.15$ mb we have $r_0 = (1.12 \pm 0.04) \times 10^{-13}$ cm. This agrees with the value $(1.01 \pm 0.06) \times 10^{-13}$ cm obtained from high energy electron scattering experiments on helium[27] and with $r_0 = (1.1 \pm 0.1) \times 10^{-13}$ cm obtained similarly for heavier elements.[28] As shown by Khokhlov[29] and Levinger,[13] taking $r_0 = 1.1$ to 1.2×10^{-13} cm also gives for heavy nuclei a value of σ_b that agrees with the experiments.

The experimentally determined moments of the photodisintegration cross section thus agree well with theoretical values calculated for electric dipole transitions by means of phenomenological sum rules including the effect of exchange forces. This indicates that electric quadrupole absorption plays a minor role in the photodisintegration of helium.

TABLE III

Photon energy Mev	$\sigma_{int} = \int_{19.8}^{E_\gamma} \sigma(W)\, dW$ (Mev. mb)	
	From our data	From the data of other authors
40	25.0±1.8	16±5 [15]
100	35.8±2.6	34 [17]
135	—	15 [20]
170	37.8±2.8	—

Levinger[30] and Khokhlov[31] also have calculated σ_{int} and σ_b for the photodisintegration of deuterium and found good agreement with the experimental values.

Angular Distributions

The angular distributions of protons from the reaction $He^4(\gamma, p)H^3$ have been derived by Daragan (private communication) for different multipolarities of photon absorption. In accordance with his results we tried to fit our angular distributions to the expression

$$A[\sin^2\theta + \beta \sin^2\theta \cos\theta + \gamma \sin^2\theta \cos^2\theta], \quad (9)$$

where the term with $\sin^2\theta$ corresponds to E_1 absorption (no spin change of the system), the term with $\sin^2\theta \cos^2\theta$ corresponds to E_2 absorption, and the term with $\sin^2\theta \cos\theta$ is due to E_1, E_2 interference.

The coefficients A, β, γ obtained by least squares fitting are given in Table IV.

One sees from Table IV that for photon energies below 30 Mev the (γ, p) reaction goes almost completely via electric dipole transitions. The absence of an isotropic component indicates that the particles leave with antiparallel spins. As mentioned earlier there occurs a sharp change in the angular distributions at $E_\gamma = 30 - 35$ Mev. For $E_\gamma = 30 - 170$ Mev the maximum of the angular distribution has moved forward to an angle $65 - 70°$. An isotropic component is absent also in this energy range. This change in the angular distribution shows that from $E_\gamma \sim 30$ Mev on electric quadrupole absorption sets in and produces the interference term $\sin^2\theta \cos\theta$. The analysis of the angular distribution indicates that the contribution of electric quadrupole absorption to the (γ, p) cross section in the energy interval $30 - 170$ Mev is around 10%. Assuming that the electric quadrupole absorption contributes with the same strength to the other processes one finds that the contribution of electric quadrupole absorption to the integrated cross section does not exceed 6%. This agrees with the above findings on the smallness of the contributions of electric quadrupole absorption obtained from the agreement of the experimental and theoretical moments of the absorption cross section.

TABLE IV

E_γ, Mev	$A\left(10^{29}\frac{cm^2}{sterad\ Q}\right)$	β	γ
21—30	7.6±0.7	0.11±0.13	—0.2±0.3
30—170	6.1±0.6	1.05±0.16	0.53±0.25

It is of interest to compare the angular distributions of the protons from the (γ, p) reaction on helium with those obtained in a (γ, p) reaction from deuterium (see Refs. 32, 33) and also from the light nuclei.[6,7] The angular distributions for deuterium are already unsymmetrical at photon energy 20 Mev. They also contain an isotropic component the magnitude of which increases with increasing photon energy.

As has been shown by Shevchenko[7] the angular distributions of fast photoprotons from light nuclei also consist of a large anisotropic and a strong isotropic component. The analysis carried out by Shevchenko shows that they agree well with the angular distributions of photoprotons from deuterium (at the equivalent proton energies). This has been interpreted as a confirmation of the pseudodeuteron effect. The absence of an isotropic component in the angular distribution of the process $He^4(\gamma, p)H^3$, perhaps, is an indication that in helium in (γ, p) and (γ, n) processes the pseudodeuteron effect is unimportant even for high photon energies.

In conclusion, the authors wish to express their gratitude to Professor P. A. Cerenkov for his continuing interest in this work, to Iu. K. Khokhlov and V. Daragan for the communication of their results, to S.

I. Shornikov, A. G. Gerasimov, V. S. Silaeva, N. N. Novikova, and K. V. Chekhova who participated in taking and processing the pictures, and to the synchrotron crew.

[1] D. Walker, Phys. Rev. 81, 634 (1951).
[2] C. Levinthal and A. Silverman, Phys. Rev. 82, 822 (1951).
[3] J. S. Keck, Phys. Rev. 85, 410 (1952).
[4] J. W. Rosengreen and J. M. Dudley, Phys. Rev. 89, 603 (1953).
[5] J. W. Weil and B. D. McDaniel, Phys. Rev. 92, 391 (1953).
[6] S. A. E. Johansson, Phys. Rev. 97, 434 (1955).
[7] I. V. Chivilo and V. Shevchenko, J. Exptl. Theoret. Phys. (U.S.S.R.) 32, 1335 (1957), Soviet Phys. JETP 5, 1090 (1957).
[8] J. S. Levinger, Phys. Rev. 84, 43 (1951).
[9] Iu. K. Khokhlov, J. Exptl. Theoret. Phys. (U.S.S.R.) 23, 241 (1952).
[10] S. Yoshida, Progr. Theoret. Phys. 6, 1032 (1951).
[11] J. S. Levinger and H. A. Bethe, Phys. Rev. 78, 115 (1950).
[12] A. B. Migdal, J. Exptl. Theoret. Phys. (U.S.S.R.) 15, 81 (1945).
[13] J. S. Levinger, Phys. Rev. 97, 122 (1955).
[14] J. C. Gunn and J. Irving, Phil. Mag. 42, 1353 (1951).
[15] E. G. Fuller, Phys. Rev. 96, 106 (1954).
[16] G. De Saussure and L. S. Osborne, Phys. Rev. 99, 843 (1955).
[17] E. R. Gaerttner and M. L. Yeater, Phys. Rev. 83, 146 (1951).
[18] T. S. Benedict and W. M. Woodward, Phys. Rev. 83, 1269 (1951).
[19] S. Kikuchi, Phys. Rev. 86, 126 (1952).
[20] V. O. Nicolai and E. L. Goldwasser, Bull. Am. Phys. Soc. 29, 18 (1954); Phys. Rev. 94, 755 (1954).
[21] Gorbunov, Spiridonov, and Cerenkov, Приборы и техника эксперимента (Instr. and Exptl. Tech.) 2, 29 (1957).
[22] Gerasimov, Gorobunov, Ivanov, Kutsenko, V. M. Spiridonov Приборы и техника эксперимента (Instr. and Exptl. Tech.) 3, 10 (1957).
[23] Barber, George, and Reagan, Phys. Rev. 98, 73 (1955).
[24] Roganov, Baranov, and Gol'danskii, J. Exptl. Theoret. Phys. (U.S.S.R.) 33, 1123 (1957), Soviet Phys. JETP (in press) (1958).
[25] J. E. Perry and S. Bame, Phys. Rev. 99, 1368 (1955).
[26] Iu. K. Khokhlov, J. Exptl. Theoret. Phys. (U.S.S.R.) 32, 124 (1957), Soviet Phys. JETP 5, 88 (1957).
[27] R. W. McAllister and R. Hofstadter, Phys. Rev. 102, 851 (1956).
[28] Hofstadter, Hahn, Kundsen, and McIntyre, Phys. Rev. 95, 512 (1954).
[29] Iu. K. Khokhlov, Dokl. Akad, Nauk SSSR 97, 239 (1954).
[30] J. S. Levinger, Phys. Rev. 97, 970 (1955).
[31] Iu. K. Khokhlov, Thesis, Physics Institute, Academy of Sciences, U.S.S.R. (1957).
[32] L. Allen, Phys. Rev. 98, 705 (1955).
[33] Aleksandrov, Delone, Slovokhotov, Sokolov, and Shtarkov, J. Exptl. Theoret. Phys. (U.S.S.R.) 33, 614 (1957), Soviet Phys. JETP (in press) (1958).

Translated by M. Danos
4